EARTHQUAKES AND ROCK CREEP

(PART I: CREEP CHARACTERISTICS OF ROCKS AND THE ORIGIN OF AFTERSHOCKS)*

By HUGO BENIOFF

INTRODUCTION

MANY seismic phenomena are adequately explained on the basis of a simple elastic theory of rock characteristics in which strain is proportional to stress and is independent of time. It is known, however, that the elastic characteristics of solids in general and rocks in particular depart greatly from these simple assumptions. It is the purpose of this paper to investigate the possible relationship of this departure to the origin of aftershocks and to the characteristics of earthquake sequences. Part I is concerned with the creep characteristics of rocks and the origin of aftershocks. Part II, which will appear at a later date, discusses earthquake sequences.

STRAIN CHARACTERISTICS OF ROCKS

If a rock sample is subjected to a continuous stress of constant amplitude beginning at the time $t = 0$, the resulting strain can be described with the help of curves such as the one shown in figure 1. For the type of response represented in this figure the stress produces an initial instantaneous elastic strain *oa* at the moment when it is applied, and this is followed by an additional strain *ab* which increases with time at a diminishing rate. If at the time corresponding to the point *b* the stress is reduced to zero, the strain recovers instantly an amount *bc* which is equal to the original instantaneous elastic strain *oa*. Thereafter the recovery continues with time and eventually the strain is reduced to zero. The part of the strain which varies with time is designated as creep. The time required for the development of a substantial part of a creep strain depends upon the characteristics of the substance as well as the stress conditions and may vary from a few minutes to possibly a century or more. For the type of creep represented by the curves in figure 1, recovery is eventually complete following release of stress, and it is therefore defined here as elastic creep. The part *ab*, which represents response to an applied stress, is designated forward creep. The part following *c*, which represents elastic afterworking, is designated creep recovery. In elastic creep the stress is always less than the strength of the material.

The curves in figure 2 represent another type of creep which can be observed with the same sample as in figure 1 by sufficiently increasing the temperature or the stress, or both, or with a different sample under the same conditions. In

* Manuscript received for publication January 18, 1950.

this type of creep the early part is substantially the same as that represented in figure 1, but thereafter the curve approaches a straight line asymptotically. Later parts therefore represent a constant strain rate or flow. This type of strain response is composed of a combination of elastic creep plus a plastic

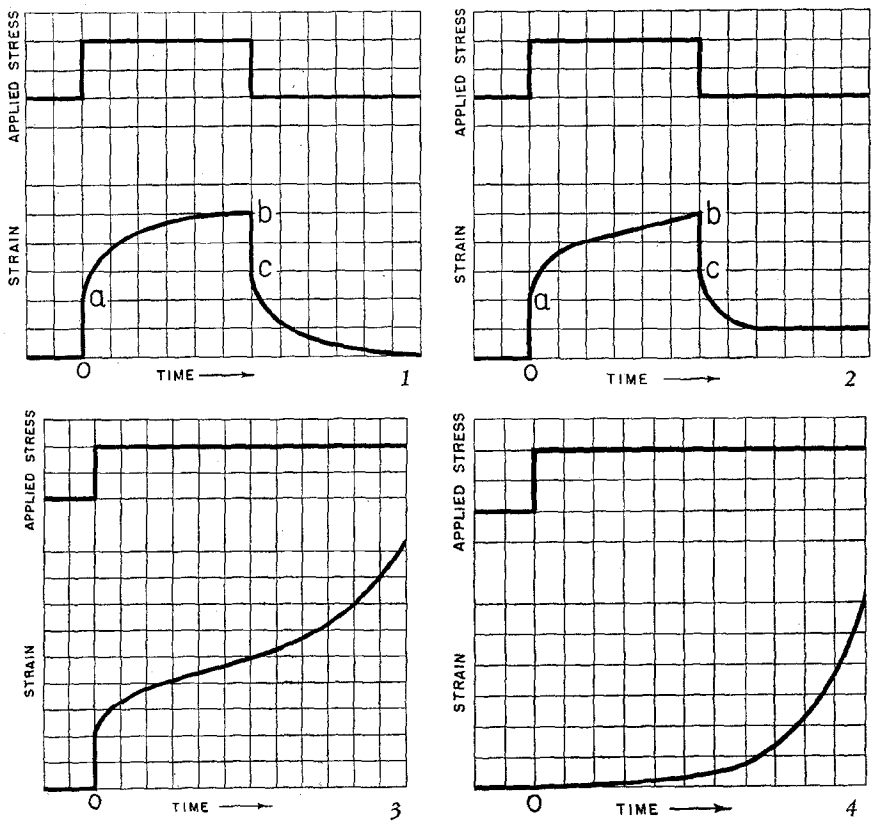

Fig. 1. Strain at constant stress in a substance having elastic creep characteristics.
Fig. 2. Strain at constant stress in a substance having elastic-flow creep characteristics. Relatively short stress cycle.
Fig. 3. Strain at constant stress in a substance having elastic-flow creep characteristics. Long stress cycle.
Fig. 4. Strain at constant stress in a substance having plastic-flow creep characteristics.

or viscous flow and is here designated elastic-flow creep. A viscous flow is one in which the strain rate is proportional to stress, whereas in plastic flow the strain rate is nonlinear with respect to stress and (or) is time-dependent. In this type of creep, release of stress as at b results in an instantaneous elastic recovery $bc = oa$ followed by an elastic creep as in the case of figure 1. Recovery, however, is not complete. The contribution resulting from flow repre-

sents a permanent deformation or set. The permanent deformation may be taken as evidence that in creep of the elastic-flow type the stress exceeds the strength of the material. On this basis strength may be defined as the greatest stress which a substance can sustain without exhibiting flow or fracture.

The curve in figure 3 represents another type of creep, which has been observed in laboratory tests of many substances, including rocks.[1] The early part of the response is similar to that of elastic-flow creep (fig. 2), but thereafter the flow component becomes curvilinear with respect to time and the rate increases continually until the sample ruptures. This type of creep is believed to be the same as elastic flow described in the preceding paragraph, the difference between the two being an effect of stress duration only. Thus if the stress is maintained for a sufficient length of time the linear flow of figure 2 eventually becomes curvilinear as in figure 3.

Elastic creep, as represented by the curve in figure 1 and the early parts of the curves in figures 2 and 3 in which the rate decreases with time, is characteristic of substances which undergo strain hardening. The hardening is presumably brought about by reorientation of the elementary particles or domains within the structure in response to the externally applied stress. The particles do not all remain indefinitely in their strained positions. Some return spontaneously to their original unstrained state. This behavior is known as annealing. The rate of annealing depends upon the temperature. At low temperatures it may be so slow as to be inappreciable for many years. With increasing temperature the annealing rate increases sharply, so that above some critical temperature it effectively prevents the occurrence of strain hardening. The creep-strain response corresponding with this condition is a flow which, at constant stress, has an increasing rate with respect to time as shown by the curve in figure 4. This type of creep is here designated plastic flow.

Although the annealing rate may be quite small at low temperatures, it is not zero (except perhaps in single crystals), and consequently with sufficient time all polycrystalline or amorphous substances can be expected to exhibit plastic flow of the type shown in figure 4 or in the later part of the curve in figure 3.

In polycrystalline or amorphous substances the concepts of strength and elastic creep are therefore valid for finite stresses of short duration only. Nevertheless, in Part II of this paper evidence from earthquake sequences is presented which indicates that crustal rocks can exhibit elastic creep without flow down to depths of 700 km. for periods of at least twenty-five years. However, for most geological processes involving stresses the time scale is so great that strength and elastic creep must appear as transient characteristics only.

[1] David Griggs, "Experimental Flow of Rocks under Conditions Favoring Recrystallization," *Bull. Geol. Soc. Am.*, 51:1002–1022 (1940); see p. 1013. P. G. McVetty, "Working Stresses for High-Temperature Service," *Mech. Engineering*, 56:149–154 (1934), and "The Interpretation of Creep Tests," *Am. Soc. for Testing Materials*, Vol. 34, Pt. II, pp. 105–116 (1934).

The behavior of a rock sample subjected to a constant stress but otherwise free from external constraints was described in the preceding paragraphs. If, instead, the sample is subjected to a suddenly applied constant strain at the time $t = 0$, the resulting stress which it exerts on its constraining structure may be represented by the curves in figures 5 and 6. Figure 5 refers to a sample

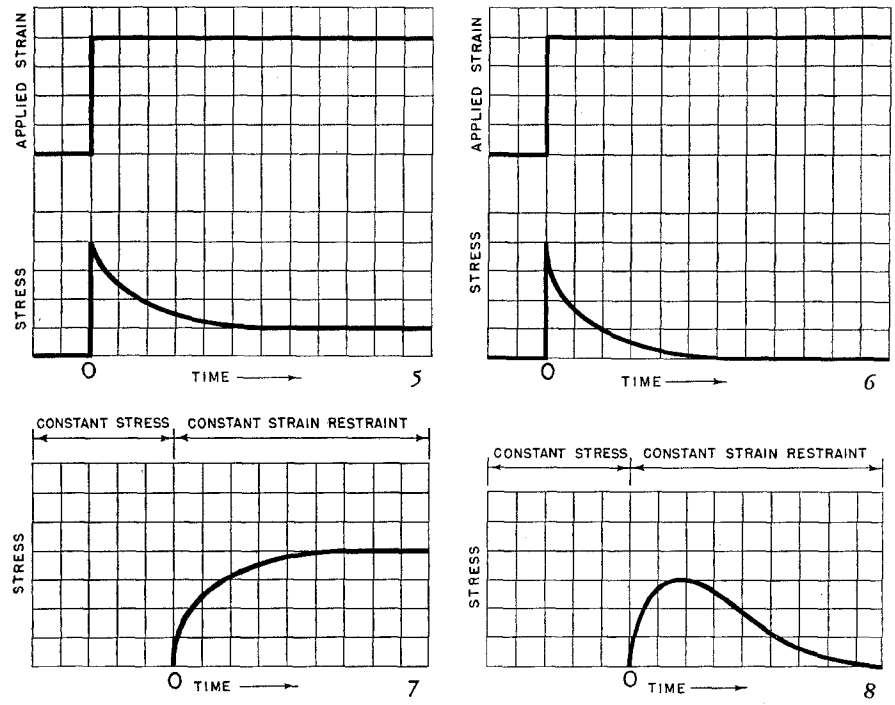

Fig. 5. Stress relaxation at constant strain in a substance having elastic-creep characteristics.

Fig. 6. Stress relaxation at constant strain in a substance having elastic-flow creep characteristics.

Fig. 7. Relaxation stress at constant restraint applied after release of constant stress in substance having elastic-creep characteristics. This curve represents the aftershock generating stress.

Fig. 8. Relaxation stress at constant strain applied after release of constant stress in substance having elastic-flow creep characteristics. May represent aftershock generating stress.

having elastic-creep characteristics. In this material, stress begins at maximum value at $t = 0$ and thereafter decreases with time, approaching asymptotically a constant value greater than zero. This phenomenon of change of stress under constant strain is known as relaxation. Figure 6 refers to a substance having elastic-flow creep characteristics. It will be noted that with this material the early part of the stress-relaxation response is the same as in the elastic-creep

material of figure 5, but in the later parts the stress decreases ultimately to zero.

Let us suppose a substance having elastic-creep characteristics is subjected to a constant stress for a time long enough to develop a substantial creep strain response as in figure 1. If at the time corresponding with the point *b* the stress is reduced to zero, and in its place a constant strain restraint is applied, the resulting stress developed within the substance by relaxation will appear as in figure 7. The stress begins at a zero value and increases at a rate which decreases with time and finally approaches a constant value. It will be shown later that aftershocks are generated by relaxation stresses of this type. In a substance having elastic-flow creep characteristics the corresponding relaxation characteristic is represented by the curve of figure 8. In this type of relaxation the stress increases from zero to a maximum value and then returns more slowly to zero.

Laboratory creep measurements are usually made with samples which have not been subjected to stress prior to the time of measurement. On the other hand, the rocks of active faults are subjected to many cycles of strain and recovery. Such repeated applications of stress with recovery produce in the strain characteristics changes known as fatigue effects. Unfortunately, very little observational material is available concerning the effects of fatigue on the creep of rocks. Moreover, available laboratory observations of fatigue in other substances are nearly always concerned with alternating stress cycles, whereas in faults the stress cycle is unidirectional, at least over periods of time covering many cycles.

Since there is no generally accepted terminology covering creep phenomena, the concepts described in the preceding paragraphs have been assembled into a set of definitions suitable for use in geophysics, as follows.

STRESS	Force per unit area.
STRAIN	Change in shape and (or) dimension of a unit quantity of a substance in response to stress.
ELASTIC STRAIN	Strain which is independent of duration of stress. It may be linear or nonlinear in relation to stress. Recovery is complete following release of stress.
CREEP	Strain which varies with duration of stress. It is usually nonlinear in relation to stress, except for viscous flow as defined below.
ELASTIC CREEP	Creep in which recovery is eventually complete following release of stress. It is usually nonlinear in relation to stress, and occurs only for stress values less than the strength.
ELASTIC FLOW	Creep in which recovery is partial following release of stress. It combines flow and elastic creep. Stress exceeds strength.
FLOW	Creep in which there is no recovery following release of stress.
VISCOUS FLOW	Flow in which the strain rate is linear in relation to stress.
PLASTIC FLOW	Flow in which the strain rate is nonlinear in relation to stress. It may vary with time at constant stress.

RELAXATION — Time-dependent stress change in response to strain increment or restraint.

STRENGTH — Greatest stress which a material can withstand without exhibiting observable flow or fracture. It varies with duration of stress in amorphous and polycrystalline materials.

CIRCUIT DIAGRAMS

Following Burgers[2] and others, we may represent the creep behavior of rocks by means of circuit diagrams analogous to those used to describe electrical phenomena. Figure 9 shows one of a number of possible schematic circuit

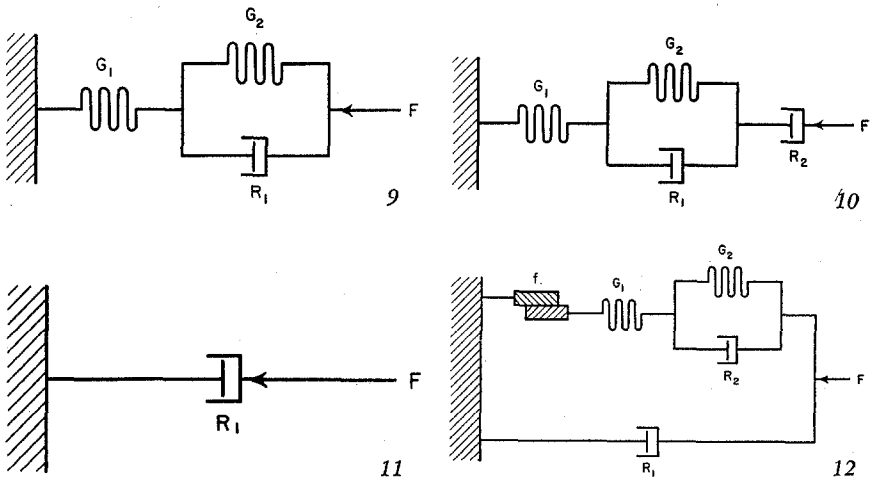

Fig. 9. Circuit diagram representing a substance having elastic creep characteristics.
Fig. 10. Circuit diagram representing a substance having elastic-flow creep characteristics.
Fig. 11. Circuit diagram representing a substance having flow characteristics.
Fig. 12. Circuit diagram representing an active fault in rock having elastic creep characteristics.

diagrams for representing an elastic-creep system having a response characteristic of the type shown in figure 1. G_1 and G_2 are elastic elements or springs. R_1 is a resistive element symbolized by a dashpot filled with a viscous liquid. F represents the applied stress.

Assume that the system is originally without stress and that at the time $t = 0$ a constant stress F is applied. The viscosity of the liquid in the dashpot prevents the piston from responding instantaneously, and consequently the full value of F is effectively exerted on G_1, producing an immediate compression corresponding to the movement *oa* in figure 1. F continues to act on R_1 and G_2, producing movement of R_1 and G_2 which begins with the velocity F/R_1 and decreases thereafter as a result of the increasing restoring force of G_2 produced

[2] J. M. Burgers, "First Report on Viscosity and Plasticity," *Acad. Sci. Amsterdam*, 1935; and Charles Mack, "Plastic Flow, Creep, and Stress Relaxation," *Jour. Appl. Physics*, 17: 1101–1107 (1946).

by its compression. The response of R_1 and G_2 is represented by the segment ab of the curve in figure 1. If at the time $t = T$ the stress F is reduced to zero, G_1 will expand immediately to its original uncompressed length, the expansion being represented by bc in figure 1. Thereafter G_2 expands at a finite decreasing rate which depends upon the restoring force of G_2 and the resistance of R.

In figure 10 is shown a circuit diagram representing an elastic-flow system. The flow element is symbolized by the series-resistive element R_2. Following application of the stress F, the response of this system begins very much like that of the elastic-creep system since in the beginning the movements of G_1, G_2, and R_1 are much greater than the movement of R_2. With the passage of time the movements of G_1 and G_2 decrease and ultimately become zero. R_2 continues to move in response to F and it thus provides the later parts of the strain curves shown in figures 2 and 3. It is clear that if F is reduced to zero, G_1, G_2, and R_1 recover exactly as in the elastic-creep system. Moreover, this recovery is transmitted through R_2 without change, since there is no external stress or constraint acting on R_2 to produce movement of the piston relative to the cylinder. The original movement of R_2 in response to F is therefore not recovered following removal of F.

The circuit of figure 11 represents a system having simple flow characteristics only. If R_1 is linear with respect to stress and is independent of time, the flow is viscous. This type of flow is very rare. In general, R_1 is curvilinear with respect to stress and in addition varies with the duration of the stress. Under such conditions the circuit represents simple plastic flow.

Empirical Creep Functions

A number of empirical functions have been formulated to describe the observed creep behavior of laboratory samples. On the basis of a series of measurements which he made on steel at constant stress and temperature continuing up to five years, S. H. Weaver[3] proposed the following equation to describe elastic flow in tension:

$$\xi = a + b \log t + ct, \tag{1}$$

in which ξ is the creep strain and a, b, and c are constants. Griggs[4] found that this equation also accurately described the elastic flow in compression of a number of rock samples which he observed. For compressional strains in rock samples having elastic creep characteristics the equation

$$\xi = a + b \log t \tag{2}$$

was shown by Griggs to represent the observed data accurately.

[3] S. H. Weaver, "The Creep Curve and Stability of Steels at Constant Stress and Temperature," *Trans. Am. Soc. Mech. Eng.*, 58:745–751 (1936).

[4] David Griggs, "Creep of Rocks," *Jour. Geol.*, 47:225–251 (1939).

Equation (2) was first used by Boltzman[5] to describe the observed creep of a wire in torsion. In view of Michelson's work on torsion,[6] it would appear that the use of this equation in torsional creep is not satisfactory.

In creep recovery of rocks in compression Griggs noted that the single equation

$$\xi = a - b \log t \tag{3}$$

represents both elastic creep and elastic flow. This results from the fact that the contribution due to flow represented by the third term in equation (2) is not recovered upon release of stress. Equations (1), (2), and (3) are discontinuous for $t = 0$. To overcome this difficulty Lyons[7] proposed a modification of equation (1) in the form

$$\xi = a + b \log (\gamma t + 1) + ct \tag{4}$$

which is continuous in the vicinity of $t = 0$ when γ is a constant. However, for most applications in geophysics equation (1) is adequate.

An equation of the form

$$\xi = a + b \log t + c \sinh at, \tag{5}$$

in which a is a constant, may perhaps represent all compressional creep strains, including curvilinear elastic flow of the type shown in figure 3. Thus when at is small, $\sinh at = at$ and equation (5) reduces to the form of equation (1). If $b = 0$, the equation represents a flow which begins as a linear function of time and eventually becomes curvilinear with respect to time. It should be emphasized, however, that equation (5) has not been experimentally verified.

A. A. Michelson[8] investigated the strain characteristics of rocks and other solid materials subjected to torsional stresses. From these experiments he derived an empirical expression for forward-shearing elastic-flow creep in the form

$$\xi = A + B [1 - \exp (- at^{\frac{1}{2}})] + Ct^{\beta} \tag{6}$$

where A, B, C, a, and β are constants which are determined by the material and stress. His values for β cluster about an average value of 0.35. He found that equation (4) also describes shearing creep recovery provided that the

[5] L. Boltzman, "Zur Theorie der elastischen Nachwirkung," *Pogg. Ann.*, Ergänzungsband 7, 624–654 (1876); *Sitz. Ber. K. Akad. Wiss. Wien, math.-naturwiss. Classe*, 70 II: 275–306 (1875).

[6] A. A. Michelson, "Elastic Viscous Flow," Part I, *Jour. Geol.*, 25:405–410 (1917); Part II, *ibid.*, 28:18–24 (1920).

[7] W. James Lyons, "The General Relations of Flow in Solids and Their Application to the Plastic Behavior of Tire Cords," *Jour. Appl. Physics*, 17:472 (1946).

[8] *Op. cit.*

constant C is zero. In shearing creep strain the term Ct^{β} must therefore represent the unrecoverable contribution of flow. It would appear from Michelson's work that no substance exhibits simple elastic creep without flow in response to shearing stresses.

An empirical relation for relaxation of compressional stress at constant deformation was given by Trouton and Rankine[9] in 1904 in the form

$$\sigma = \sigma_1 - B \log (\gamma t + 1) \tag{7}$$

in which σ_1, B, and γ are constants. This equation appears unsatisfactory for values of t which make $B \log (\gamma t + 1)$ greater than σ_1. Trouton and Rankine suggested that equation (7) is also valid for torsional relaxation.

Creep Theory of Aftershocks

In accordance with Reid's elastic rebound theory it will be assumed that earthquakes are produced by the sudden release of energy stored as elastic strain in the rock masses of a fault. The earthquake-producing mechanism may then be represented by a circuit diagram such as the one shown in figure 12, in which f is the fault, G_1, G_2, and R_2 are the elastic and creep elements of the fault rock, F is the earthquake-generating stress (assumed constant), and R_1 is a secular resistive element which is characteristic of the medium in which F originates and which with F determines the secular rate of strain accumulation.

Let us assume that, following an earthquake, G_1 and G_2 are completely relaxed and that the surfaces of the fault f have become locked by friction and (or) cementing. The system G_1 G_2 R_1 R_2 is slowly compressed at a rate determined mainly by the ratio of F, the generating stress, to R_1, the secular resistive element. It is further assumed that $R_1 > R_2$. The elastic compression of G_1 and G_2 exerts a stress on the fault f which increases at a secular rate until the moment when the stress at some point along the fault exceeds the cohesive strength of the fault and thus initiates slippage at the particular point. This in turn increases the stress at neighboring points, and thus a faulting movement is propagated along the length of the fault with a velocity less than that of longitudinal waves. Once movement has begun, the static friction of the fault changes to the much smaller dynamic friction, and slipping continues until the elastic strain of G_1 is very nearly reduced to zero. In the short interval during which the fault is in motion—less than two minutes—elements R_1 and R_2 are unable to respond appreciably, and consequently at the conclusion of the fault movement G_2 remains fully strained. The energy of the principal earthquake is thus derived solely from the quick-acting elastic element G_1. It

[9] F. T. Trouton and A. O. Rankine, "On the Stretching and Torsion of Lead Wire beyond the Elastic Limit," *Phil. Mag.* Ser. 6, 8; 538–556 (1904).

will be assumed that immediately after the fault comes to rest the surfaces again become locked by virtue of the increased static friction, but that as a result of reduced normal stress and cementing the threshold value of stress required to initiate motion is less than that which gives rise to the principal earthquake. With the release of G_1 by the earthquake the full stress of the compressed G_2 is effective across the frictional element R_2 and therefore produces a strain recovery of R_2 and G_2 with a rate which starts at maximum and decreases thereafter. As a result of the high friction of R_1 its movement is too slow to be effective except over long intervals of time, and consequently movement of the elements G_2 and R_2 produces a compression of G_1 which increases

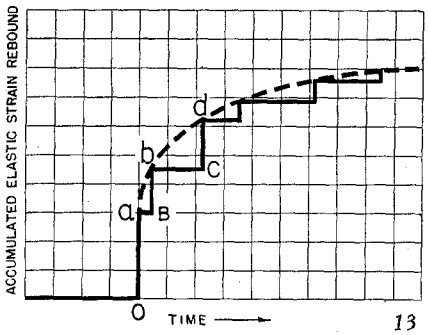

Fig. 13. Elastic strain rebound increments associated with an earthquake and its aftershocks.

with time. Locking of the fault after the elastic release of G_1 during the earthquake thus provides a strain restraint to the fault rock of the type discussed in connection with the relaxation curve of figure 5. Consequently the resulting compression of G_1 symbolizes the relaxation stress of the fault rock. This stress exerts a force on the locked fault surfaces f which increases with time as shown in the relaxation curve of figure 5. When this force increases to a value such that the stress at some point on the fault exceeds the local frictional strength, the fault slips again and thus generates the first aftershock. When the slipping movement ceases, the fault locks again and the relaxation process is repeated. In this way a sequence of aftershocks is produced which continues until the strain in G_2 is relieved. The size of any particular aftershock is determined by the amount of the fault-locking friction at the moment that movement begins. Since the fault surfaces may be assumed to be very rough, the locking friction varies from shock to shock, with the result that the aftershocks, and the elastic strain-rebound increments which generate them, vary in size. If the accumulated sum of rebound increments is plotted against the time, as in figure 13, the resulting curve is made up of a series of vertical and horizontal segments. The fault is at rest up to the time $t = 0$, when it rebounds elastically

a strain increment oa to produce the principal earthquake. Following the principal shock the fault remains stationary until the occurrence of the first aftershock during which the total elastic rebound strain increases by the increment Bb. The quiescent interval between the first and second aftershocks is represented by bC. The fault-rebound strain increment occurring during the second aftershock is Cd, and so on. If each aftershock reduces the instantaneous strain of G_1 to zero, the dotted curve joining the points $a, b, d, \cdots n$ represents approximately the creep recovery curve of the fault rock. If the fault rock has an elastic-creep characteristic, the approximation is close. If the creep characteristic of the rock is of the elastic-flow type, then the dotted curve represents the creep recovery minus the relaxation flow which occurs during the intervals when the fault is locked.

It should be emphasized that the immediate source of energy of the principal shock as well as that of the aftershocks is the quick-releasing elastic strain of the element G_1. However, the energy released from G_1 in aftershocks represents energy stored originally in the slowly acting creep element G_2. The efficiency of transfer of energy from G_2 to G_1 depends upon the size of an aftershock. When the shock is small, G_1 is only slightly strained and consequently most of the work done by G_2 in expanding is used up in producing movement of R_2 and appears as heat in R_2. When the shock is larger, G_1 presents an increased restoring force, and a larger proportion of the work done by G_2 is used up against this greater restoring force, with a consequent increase in efficiency of energy transfer. Although the efficiency of transfer varies with size of shock and thus makes energy an unreliable basis for studying earthquake creep phenomena—at least without efficiency corrections,—the elastic strain of G_1 preceding an aftershock is always equal to the creep strain recovery increment of G_2 which produces it. Consequently, in a series of aftershocks, if a way can be found for calculating the strains of G_1, it will provide the necessary information with which to construct a creep curve of the fault rock.

Consider an elementary volume dv, situated within the strained fault rock. The energy of elastic strain stored in dv is

$$dW = \tfrac{1}{2}\mu\epsilon_1^2 dv\,. \tag{8}$$

μ is an elastic constant and ϵ_1 is the strain. The equation is valid for any type of strain, provided the appropriate values for μ and ϵ_1 are chosen. If the total volume of strained rock is A, the total stored elastic energy is

$$W = \int_0^A \tfrac{1}{2}\mu\epsilon_1^2 dv \text{ ergs}\,. \tag{9}$$

In general the distribution of the strain pattern within the rock mass is unknown, and consequently equation (9) cannot be integrated. However, an

equivalent system may be postulated in which the strain has an average constant value ϵ throughout a volume V of rock. Equation (9) can be integrated for this system and the total energy is thus

$$W = \tfrac{1}{2}\mu\epsilon^2 V \text{ ergs}. \tag{10}$$

W represents the elastic energy stored in the quick-acting element G_1 in the circuit diagram of figure 12. When the fault slips and thus produces an earthquake, part of this stored energy is converted into seismic waves. The rest is converted into heat by the friction of the fault surfaces and other loss mechanisms in the elastic system. Let p be the fraction of stored energy which is converted into seismic waves. Then

$$J = pW = \tfrac{1}{2}\mu p\epsilon^2 V \text{ ergs} \tag{11}$$

is the total energy radiated in the form of waves.

Extracting the square root of equation (11) we have

$$J^{\frac{1}{2}} = \epsilon\,(\tfrac{1}{2}\mu p V)^{\frac{1}{2}}\,(\text{ergs})^{\frac{1}{2}}. \tag{12}$$

For any given fault system p is constant and nearly equal to unity, and consequently the quantity under the radical may be considered constant. Thus

$$\tfrac{1}{2}\mu p V = k^2 \tag{13}$$

and

$$J^{\frac{1}{2}} = k\epsilon\,(\text{ergs})^{\frac{1}{2}} \tag{14}$$

Thus, in a given fault system, if the elastic strain is fully relieved during fault movement, the square root of the radiated energy of an earthquake is proportional to the elastic strain (preceding the earthquake) of the element G_1 of the fault rock. Consequently, in a series of aftershocks the values of $J^{\frac{1}{2}}$ for the separate shocks represent creep strain recovery increments of the fault rock, and a graph of the accumulated sum of these increments plotted against time represents very nearly the creep strain recovery curve of the rock (multiplied by the constant k), that is,

$$S = \sum J_i^{\frac{1}{2}} = \sum k\epsilon_i = k\xi \tag{15}$$

where ξ is the creep strain recovery.

The most accurate available means for determining the energy of earthquakes is provided by the modified magnitude scale of Gutenberg and Rich-

ter.[10] They give the following equation for the relation between the energy J and the magnitude M (the constant term is revised in accordance with their latest determination):

$$\log J = 12.0 + 1.8\,M \text{ ergs} \tag{16}$$

Hence

$$\log J^{\frac{1}{2}} = 6.0 + 0.9\,M\,(\text{ergs})^{\frac{1}{2}} \tag{17}$$

Aftershock Sequence of the Long Beach Earthquake

The epicenter of the Long Beach, California, earthquake of March 10, 1933 ($\phi = 33° 34'.5$ N; $\lambda = 117° 59'$ W), was favorably situated within the network of stations of the California Institute of Technology for aftershock study. Dr. Richter made available to me an unpublished list of aftershock magnitudes which he computed from measurements of the Haiwee seismograms compiled by H. O. Wood. His list includes all shocks of magnitude 3.9 and greater which occurred within a ten-day interval following the principal shock. Mr. Ralph Gilman of the laboratory staff extended the list to include all shocks in the same magnitude range to October 2, 1933. The extended list is given in table 1. The origin times, t, of the aftershocks are measured in days from the origin time of the principal shock, which is taken as March 10, 1933, 17:54:08 P.S.T. For any particular aftershock, S is the sum of the increments $J^{\frac{1}{2}}$ for the shocks which occurred in the interval, beginning with the first aftershock and ending with the particular shock. It may be assumed, therefore, that S represents the creep strain recovery multiplied by the constant k.

Figure 14 is a graph of S in semilog coördinates as a function of the time in days measured from the origin time of the principal earthquake. The value of S for each aftershock is represented by a dot having a diameter related to the magnitude as shown in the legend in the figure. It will be noted that the dots fall on two distinct curves. One curve begins with the first aftershock at $t = 0.007$ day and continues to $t = 0.15$. This curve is calculated from the equation

$$S_i = [4.07 + 1.82 \log t] \times 10^{11}\,(\text{ergs})^{\frac{1}{2}}. \tag{18}$$

It represents a compressional elastic-creep strain as defined by equation (2) or equation (3). Since the increments of S are derived from the square root of the energy, their signs are indeterminate. It is thus impossible from these measurements alone to distinguish between forward creep as represented by equation (2) and creep recovery as represented by equation (3). In accordance with the theoretical considerations discussed earlier, it may be assumed that

[10] B. Gutenberg and C. F. Richter, "Earthquake Magnitude, Intensity, Energy, and Acceleration," *Bull. Seism. Soc. Am.*, 32:163–191 (1942).

TABLE 1

AFTERSHOCK SEQUENCE, LONG BEACH EARTHQUAKE, MARCH 10, 1933

Date	Origin time, P.S.T.	t	M	$J^{1/2}$	S	J_i
				$\times 10^{10}$	$\times 10^{10}$	$\times 10^{20}$
March 10	18:05	0.00764	4.8	2.00	2.00	4.0
	18:10	.0111	4.9	2.50	4.50	6.3
	18:11	.0118	4.6	1.40	5.90	2.0
	18:17	.0160	4.7	1.80	7.70	3.2
	18:22	.0194	3.9	0.32	8.02	0.1
	18:28	.0236	4.6	1.40	9.42	2.0
	18:30	.0250	5.0	3.20	12.62	10.0
	18:44	.0347	4.6	1.40	14.02	2.0
	19:06	.0500	4.2	0.63	14.65	0.4
	19:09	.0520	4.4	0.89	15.54	0.8
	19:11	.0535	4.2	0.63	16.17	0.4
	19:24	.0625	4.9	2.50	18.67	6.3
	19:33	.0686	3.9	0.32	18.99	0.1
	19:36	.0708	3.9	0.32	19.31	0.1
	19:40	.0736	3.9	0.32	19.63	0.1
	20:37	.113	4.6	1.40	21.03	2.0
	21:11	.137	5.1	4.00	25.03	16.0
	21:15	.139	4.7	1.80	26.83	3.2
	21:18	.1415	5.2	5.00	31.83	25.0
	21:21	.1435	4.4	0.89	32.72	0.8
	21:25	.1465	4.2	0.63	33.35	0.4
	21:54	.1665	3.9	0.32	33.67	0.1
	21:55	.1675	3.9	0.32	33.99	0.1
	22:12	.179	4.4	0.89	34.88	0.8
	22:18	.183	4.2	0.63	35.51	0.4
	22:30	.1915	4.4	0.89	36.40	0.8
	23:02	.214	5.4	7.10	43.50	50.0
	23:52	0.249	4.2	0.63	44.13	0.4
March 11	00:09	0.261	4.5	1.10	45.23	1.3
	00:32	.278	4.2	0.63	45.86	0.4
	00:37	.280	3.9	0.32	46.18	0.1
	00:55	.293	5.0	3.20	49.38	10.0
	01:10	.303	5.0	3.20	52.58	10.0
	01:22	.311	4.4	0.89	53.47	0.8
	02:46	.368	3.9	0.32	53.79	0.1
	03:01	.380	3.9	0.32	54.11	0.1
	03:04	.382	4.6	1.40	55.51	2.0
	03:29	.399	3.9	0.32	55.83	0.1
	03:38	.405	4.2	0.63	56.46	0.4
	03:47	.411	4.4	0.89	57.35	0.8
	04:50	.456	4.4	0.89	58.24	0.8
	05:51	.497	4.4	0.89	59.13	0.8
	05:58	.502	3 9	0.32	59.45	0.1
	06:26	.522	4 9	2.50	61.95	6.3

TABLE 1—*Continued*

Date	Origin time, P.S.T.	t	M	$J^{1/2}$	S	J_i
				$\times 10^{10}$	$\times 10^{10}$	$\times 10^{20}$
March 11— *Continued*	06:48	0.537	4.4	0.89	62.84	0.8
	06:57	.544	4.9	2.50	65.34	6.3
	07:10	.552	4.4	0.89	66.23	0.8
	08:54	.625	4.8	2.00	68.23	4.0
	11:56	.750	4.2	0.63	68.86	0.4
	14:00	.843	4.4	0.89	69.75	0.8
	14:31	.858	4.4	0.89	70.64	0.8
	14:40	.868	4.4	0.89	71.53	0.8
	15:06	.882	4.2	0.63	72.16	0.4
	16:28	0.94	4.4	0.89	73.05	0.8
	21:47	1.161	4.4	0.89	73.94	0.8
	22:01	1.171	4.2	0.63	74.57	0.4
	22:17	1.182	4.6	1.40	75.97	2.0
March 12	07:02	1.550	4.2	0.63	76.60	0.4
	10:25	1.685	4.0	0.40	77.00	0.1
	15:54	1.930	4.5	1.10	78.10	1.3
	20:33	2.110	4.7	1.80	79.90	3.2
	22:18	2.183	3.9	0.32	80.22	0.1
March 13	05:18	2.472	5.2	5.00	85.22	25.0
	11:30	2.731	4.2	0.63	85.85	0.4
	16:37	2.94	4.2	0.63	86.48	0.4
March 14	04:19	3.435	4.5	1.10	87.58	1.3
	11:02	3.710	5.0	3.20	90.78	10.0
	20:33	4.110	4.0	0.40	91.18	0.2
	21:41	4.160	4.2	0.63	91.81	0.4
March 15	03:14	4.390	4.9	2.50	94.31	6.3
March 16	07:30	5.570	4.2	0.63	94.94	0.4
March 18	12:52	7.80	4.2	0.63	95.57	0.4
March 19	13:24	8.79	3.9	0.32	95.89	0.1
March 20	05:58	9.30	4.2	0.63	96.52	0.4
	19:27	10.04	4.1	0.50	97.02	0.2
March 25	06:47	14.54	4.1	0.50	97.52	0.2
March 30	04:25	19.41	4.4	0.89	98.41	0.8
May 16	12:59	66.8	4.0	0.45	98.98	0.1
				$S_{max}=99\times10^{10}\,\Sigma J_i=2.4\times10^{22}$		

the creep is one of recovery. The circuit diagram of figure 12 represents the fault system of this compressional elastic-creep phase.

The second phase in the sequence begins at $t = 0.15$ day and continues to approximately $t = 70$ days. The second curve is calculated from the equation

$$S_2 = [2.5 + 7.4\{1 - \exp(-1.15T^{\frac{1}{2}})\}] \times 10^{11} \text{ (ergs)}^{\frac{1}{2}} \tag{19}$$

$$T = t - 0.135 \text{ days},$$

which is of the form of equation (6) derived by Michelson for shearing creep recovery. The circuit of figure 12 represents the fault behavior of this phase also, provided that shear values of the circuit elements are substituted for the compression values required in the first phase.

The origin of the aftershock sequence of the Long Beach earthquake may therefore be attributed to elastic afterworking of the fault rock. The afterworking began as a compressional creep strain recovery followed after an interval of 0.135 day by a shearing creep strain recovery. That there would be both compressional and shearing creep effects is not unexpected, but the delay in onset of the shearing creep strain recovery is surprising. If compressional and shearing creep strains interact with each other, it is possible that the frictional component of the shearing creep mechanism may be increased to the point of locking by action of the compressional creep stress. Thus, during relaxation, recovery of the shearing creep strain may be delayed until the compressional creep stress is reduced. Bridgman's[11] recent discovery of an anomalous volume change in rocks subjected to simple compression in the creep range of stress provides the basis for a possible mechanical explanation of the interaction between compressive and shearing creep strains. He found that up to a limiting value of compressive stress the length and volume both decrease with increasing stress increments in accordance with ordinary experience. For stresses beyond this limit the length continues to decrease but the volume increases sharply. Moreover, a substantial part of this volume increase is recoverable upon release of stress. Thus, during the initial stages of release the volume decreases. Such an anomalous behavior must involve significant changes in the internal structural configuration of the material and so exert an appreciable effect on the shearing response. The increased pressure and the changes in structure may both conspire to lock the shearing strain until the compressive stress decreases to the point where the volume changes become normal. At the moment when the shearing strain recovery began, the compressional creep ceased abruptly in spite of the fact that its rate of activity was large. Such discontinuities in creep recovery have not been

[11] P. W. Bridgman, "Volume Changes in the Plastic Stages of Simple Compression," *Jour. Appl. Physics*, 20:1241–1251 (1949).

observed in the laboratory. Moreover, in those aftershock sequences described later which were derived wholly from compressional creep strains, recovery was observed to continue for much longer intervals. It appears, therefore, that a substantial part of the original compressional creep strain is not accounted for in the recovery of this sequence. Perhaps 0.135 day after the strain re-

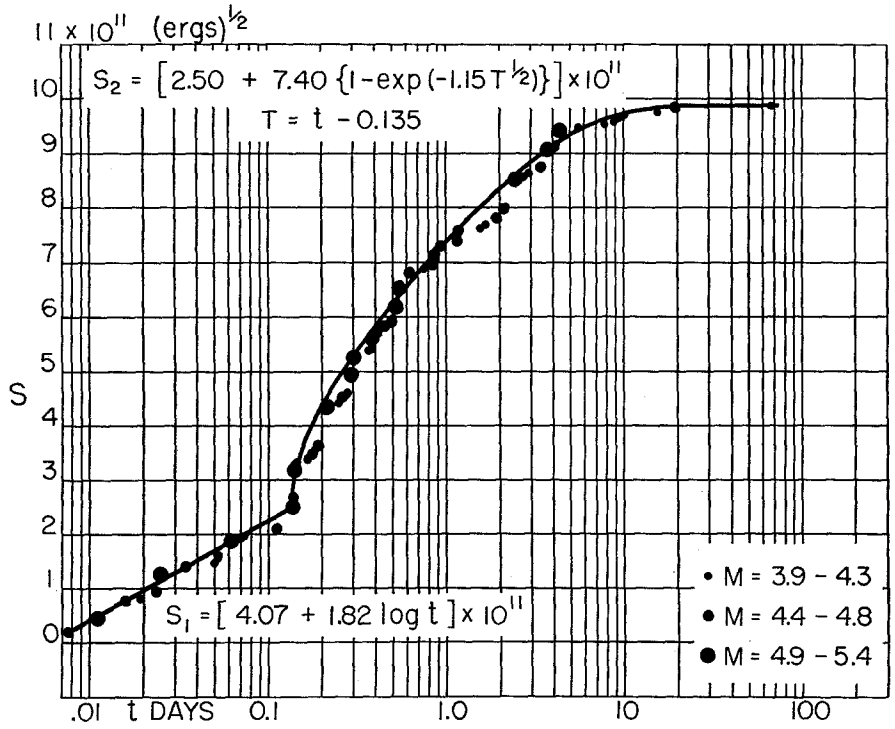

Fig. 14. Accumulated elastic strain rebound increments (times k) of the Long Beach aftershock sequence.

covery began the stress pattern of the fault allowed the compressional recovery to take place continuously without producing shocks.

It may be assumed that the purely elastic strain which produced the principal earthquake involved a combination of compressional and shearing components. The relative amounts of the two cannot be determined from these observations, partly because we do not know the relation between creep strain and elastic strain for a given substance, and partly because of the lost part of the compressional strain recovery mentioned earlier.

The total wave energy released in the aftershocks was

$$\sum J_i = 2.4 \times 10^{22} \text{ ergs}.$$

The energy released in the principal shock, which was assigned the magnitude 6.3 by Gutenberg and Richter, was

$$J_0 = 2.0 \times 10^{23} \text{ ergs.}$$

The aftershock wave energy thus amounted to only 0.12 of the principal shock energy. On the other hand, the elastic strain rebound (times k) for the principal shock was

$$J_0^{\frac{1}{2}} = 4.5 \times 10^{11} \text{ (ergs)}^{\frac{1}{2}}$$

whereas the total elastic strain rebound (times k) of the aftershocks was

$$S_{\max} = 9.9 + 10^{11} \text{ (ergs)}^{\frac{1}{2}}$$

or 2.2 times that of the principal shock. Thus, referring to figure 12, at the moment when the principal movement began, the strain of the creep elastic element G_2 was at least 2.2 times the strain in G_1 which produced the principal earthquake. Moreover, up to the moment when the principal movement began, the stress on G_1 was equal to the stress on G_2. By assuming a linear relationship between stress and strain one may obtain an approximate value for the energy stored in the creep-elastic element G_2. Thus, if μ_2 and ϵ_2 are the elastic constants and maximum strain of G_2, respectively, the energy stored in G_2 just before the principal earthquake occurred was

$$W_2 = \tfrac{1}{2}\mu_2\epsilon_2^2 V .$$

The energy stored in the elastic element G_1 which produced the principal earthquake was, from equation (10),

$$W = \tfrac{1}{2}\mu\epsilon^2 V .$$

Solving the two preceding equations for W_2, the energy stored in the creep-elastic element G_2, we obtain

$$W_2 = W \frac{\tfrac{1}{2}\mu_2\epsilon_2^2 V}{\tfrac{1}{2}\mu\epsilon^2 V} = W \frac{\mu_2\epsilon_2^2}{\mu\epsilon^2} .$$

Since the stress F acted equally on G_1 and G_2, we may write

$$\mu_2\epsilon_2 = \mu\epsilon = F$$

and consequently

$$W_2 = W \frac{\epsilon_2}{\epsilon} .$$

From equation (4)

$$\epsilon = J^{\frac{1}{2}}/k\,,$$

and if p is the same in the aftershocks as it is in the principal shock, then

$$\epsilon_2 = S_{\max}/k\,.$$

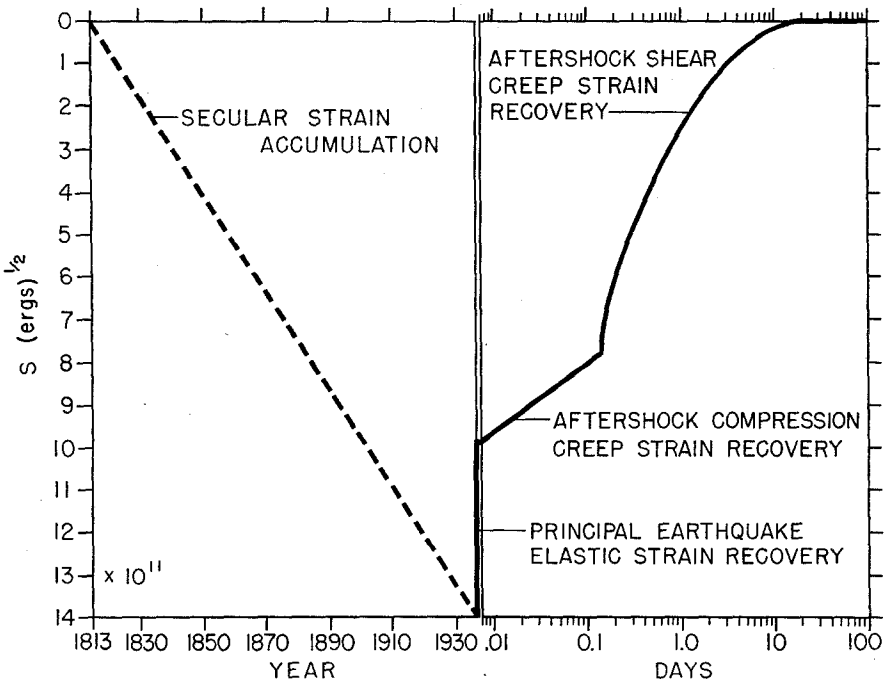

Fig. 15. Cycle of strain accumulation and recovery in the fault rock of the Long Beach earthquake.

Hence

$$W_2 = W\frac{S_{\max}}{J^{\frac{1}{2}}}\,.$$

Substituting the observed values for S max and $J^{\frac{1}{2}}$, we obtain

$$W_2 = 2.2W\,.$$

The energy stored in the creep-elastic element, which produced the aftershock sequence, was 2.2 times the energy stored in the purely elastic element and

which produced the principal earthquake. The conversion efficiency of the aftershock mechanism is

$$\frac{\sum J_1}{J_0} \Big/ \frac{Wa}{W} = \frac{0.12}{2.2} = .055 .$$

Thus, of the energy stored in the creep-elastic element, 94 per cent or 4.2×10^{23} ergs was dissipated as heat in R_2 during the twenty days of aftershock activity. This was more than twice the amount of energy released by the principal earthquake as seismic waves.

Apparently the last destructive earthquake which occurred in the Long Beach area before 1933 was the shock of December 8, 1812. Assuming that there were no other significant shocks in this area during the interval, a curve showing the cycle of strain accumulation and release for the Long Beach system can be constructed as shown in figure 15. The secular strain accumulation is assumed to increase linearly with the time and is represented by a dotted line in order to indicate that the actual shape is unknown. During the principal earthquake of 1933 an elastic-strain recovery of the relative amount, shown by the vertical part of the curve, took place within an interval of approximately 10 seconds. The compressional and shearing creep recoveries followed in succession as described earlier. Thus the whole secular strain which required 120 years to accumulate was released in approximately 20 days.

Aftershock Sequence of the Hawke's Bay Earthquake

The Hawke's Bay, New Zealand, earthquake of February 3, 1931 ($\phi = 39°.5$ S, $\lambda = 177°$ E), was followed by an aftershock sequence which was recorded by a Wood-Anderson torsion seismograph in Wellington. Epicenters and maximum recorded amplitudes derived from these seismograms were listed for this sequence by Adams, Barnett, and Hayes.[12] From these data Mr. Gilman calculated the magnitudes and other entries shown in table 2. Several of the stronger aftershocks were recorded at Pasadena. A comparison of magnitudes determined from the Pasadena seismograms with those derived from the Wellington records indicated that the Wellington magnitudes were systematically too small by approximately 0.2 of a magnitude. Accordingly, the values shown in table 2 include a correction of +0.2 of a magnitude. After the curves were drawn, it was learned that the Wellington seismograph was operating with half the magnification (1,400) of the corresponding Pasadena instruments (2,800). This would account for a difference of 0.3 of a magnitude. The magnitude of the principal earthquake as determined by Gutenberg was 7.6.

Figure 16 shows a graph of S for this sequence drawn on a semilog coördinate

[12] C. E. Adams, M. A. F. Barnett, and R. C. Hayes, "Seismological Report of the Hawke's Bay Earthquake of 3 February, 1931," *New Zealand Journal of Science and Technology*, July, 1933, pp. 93–107.

TABLE 2

AFTERSHOCK SEQUENCE, HAWKE'S BAY EARTHQUAKE, 1931 FEBRUARY 3, 10:16:43 N.Z.M.T.

Date	Origin Time, N.Z.M.T.	t	M	$J^{1/2}$	S	J_i
				$\times 10^{11}$	$\times 10^{11}$	$\times 10^{21}$
1931 Feb. 3	10:25:00	0.006	5.5	0.89	0.89	7.90
	10:27:00	0.008	5.9	2.00	2.89	40.00
	11:22:45	0.034	5.4	0.71	3.60	5.00
	11:41:10	0.056	4.9	0.25	3.85	0.63
	12:55:34	0.110	4.8	0.20	4.05	0.40
	13:01:09	0.115	5.1	0.40	4.45	1.60
	13:25:21	0.131	5.0	0.32	4.77	1.00
	13:40:11	0.142	5.2	0.50	5.27	2.50
	17:16:00	0.291	5.1	0.40	5.67	1.60
	17:59:03	0.322	4.9	0.25	5.92	0.63
	20:10:54	0.412	5.2	0.50	6.42	2.50
Feb. 4	00:03:46	0.574	4.8	0.20	6.62	0.40
	01:45:48	0.646	5.2	0.50	7.12	2.50
	16:15:14	1.25	5.3	0.56	7.68	3.20
Feb. 5	01:35:05	1.54	5.3	0.56	8.24	3.20
	05:47:06	1.81	4.5	0.11	8.35	0.13
	14:07:05	2.16	4.2	0.06	8.41	0.04
	20:27:06	2.42	5.9	2.00	10.41	40.00
	22:08:47	2.49	4.3	0.07	10.48	0.05
Feb. 6	02:02:29	2.65	4.2	0.06	10.54	0.04
	10:02:12	2.99	4.2	0.06	10.60	0.04
	23:00:01	3.53	4.2	0.06	10.66	0.04
Feb. 7	10:57:39	4.03	4.5	0.11	10.77	0.13
	11:43:19	4.06	4.6	0.14	10.91	0.20
	15:35:12	4.21	5.0	0.32	11.23	1.00
	21:37:52	4.46	5.1	0.40	11.63	1.60
Feb. 8	13:13:57	5.12	5.8	1.60	13.23	25.00
	18:50:53	5.36	4.7	0.18	13.41	0.32
	21:41:04	5.47	5.4	0.71	14.12	5.00
Feb. 9	08:11:11	5.91	5.1	0.40	14.52	1.60
	13:06:51	6.12	4.5	0.11	14.63	0.13
Feb. 10	03:59:29	6.73	4.6	0.14	14.77	0.20
Feb. 11	04:44:47	7.77	4.7	0.18	14.95	0.32
	04:50:43	7.78	4.9	0.25	15.20	0.63
	11:45:21	8.06	4.2	0.06	15.26	0.04

Continued

TABLE 2—*Continued*

Date	Origin Time, N.Z.M.T.	t	M	$J^{1/2}$	S	J_i
				$\times 10^{11}$	$\times 10^{11}$	$\times 10^{21}$
Feb. 12	04:32:45	8.75	5.9	2.00	17.26	40.00
Feb. 13	12:57:21	10.1	6.9	16.00	33.26	2500.00
	13:24:41	10.1	5.0	0.32	38.58	1.00
	15:28:05	10.2	4.2	0.06	33.64	0.04
	21:19:16	10.5	4.7	0.18	33.82	0.32
	23:18:06	10.6	4.3	0.07	33.89	0.05
Feb. 14	01:12:21	10.6	4.4	0.09	33.98	0.08
	03:10:09	10.7	4.2	0.06	34.04	0.04
	08:27:56	10.9	4.4	0.09	34.13	0.08
	11:50:05	11.1	4.2	0.06	34.19	0.04
	13:50:05	11.2	4.4	0.09	34.28	0.08
Feb. 15	02:24:58	11.7	4.1	0.05	34.33	0.02
	09:06:51	12.0	4.5	0.11	34.44	0.13
	17:35:48	12.3	4.3	0.07	34.51	0.05
	17:47:55	12.3	4.7	0.18	34.69	0.32
Feb. 18	04:35:00	14.8	4.5	0.11	34.80	0.13
	19:13:10	15.4	4.5	0.11	34.91	0.13
Feb. 21	01:27:21	17.6	5.6	1.10	36.01	13.00
Feb. 22	01:09:41	18.6	4.5	0.11	36.12	0.13
Feb. 24	19:56:15	21.4	4.9	0.25	36.37	0.63
Feb. 25	11:12:50	22.0	5.4	0.71	37.08	5.00
Feb. 26	11:05:33	23.0	4.2	0.06	37.14	0.04
	20:51:00	23.4	4.5	0.11	37.25	0.13
Feb. 27	06:55:14	23.8	4.5	0.11	37.36	0.13
Mar. 1	04:16:41	25.8	4.5	0.11	37.47	0.13
	06:01:20	25.9	4.2	0.06	37.53	0.04
Mar. 8	23:20:32	33.5	6.1	3.20	40.73	100.00
Mar. 13	09:05:29	37.9	4.1	0.05	40.78	0.02
Apr. 22	11:10:14	47.0	6.3	4.50	45.28	200.00
	11:19:44	47.0	4.7	0.18	45.46	0.32
	12:01:05	47.0	4.4	0.09	45.55	0.08

TABLE 2—*Concluded*

Date	Origin time, N.Z.M.T.	t	M	$J^{1/2}$	S	J_i
				$\times 10^{11}$	$\times 10^{11}$	$\times 10^{21}$
Apr. 24	05:23:53	48.8	5.0	0.32	45.87	1.00
Apr. 26	18:37	51.3	4.4	0.09	45.96	0.08
May 14	20:20:57	69.4	5.1	0.40	46.36	1.60
May 21	16:19:03	76.2	4.4	0.09	46.45	0.08
June 10	04:25:55	95.8	5.0	0.32	46.77	1.00
June 22	03:37:06	108	4.5	0.11	46.88	0.13
	07:32:08	108	4.5	0.11	46.99	0.04
Aug. 11	04:25:21	158	4.2	0.06	47.05	0.04
Sept. 9	21:40:03	198	4.1	0.05	47.10	0.02
Sept. 12	09:53:02	201	5.7	1.40	48.50	20.00
1932 Jan. 2	12:30:00	313	4.1	0.05	48.55	0.25
Feb. 10	03:41:00	352	4.4	0.09	48.64	0.08
Apr. 21	01:29:00	423	4.4	0.09	48.73	0.08
May 5	19:54:5	437	5.8	1.60	50.33	25.00
	19:59:30	437	4.1	0.05	50.38	0.02
	23:01:00	437	4.5	0.11	50.49	0.13
June 18	02:07:30	480	5.1	0.40	50.89	1.60
June 28	21:52:53	491	4.4	0.09	50.98	0.08
				$S_{max}=5.1\times10^{12}$		$\Sigma J_i=3.1\times10^{24}$

net. The curves represent a dual creep pattern similar to that of the Long Beach sequence except that the rate of recovery in the Hawke's Bay sequence is much slower than that of Long Beach. The compressional phase lasted 2.4 days, as compared with 0.135 day for Long Beach. The shearing phase lasted approximately 500 days, as compared with 20 days for the Long Beach sequence. The total rebound strain (times k) of the aftershock sequence was $S_{max} = 5.1 \times 10^{12}$ (ergs)$^{\frac{1}{2}}$ and in the principal shock it was 6.9×10^{12} (ergs)$^{\frac{1}{2}}$. The ratio of the two is 0.74. Hence at the time of the earthquake the creep

strain of the fault rock was at least three-fourths as large as the elastic strain. The seismic wave energy released in the aftershocks and in the principal earthquake was 3.1×10^{24} and 5.0×10^{25} ergs respectively. The ratio of aftershock energy to that of the principal shock is 0.06. Assuming a linear relation between the stress and strain in the creep mechanism, the energy stored in the creep mechanism was 3.7×10^{25} ergs, of which 3.4×10^{25} ergs was released as heat during the time the aftershock sequence was active.

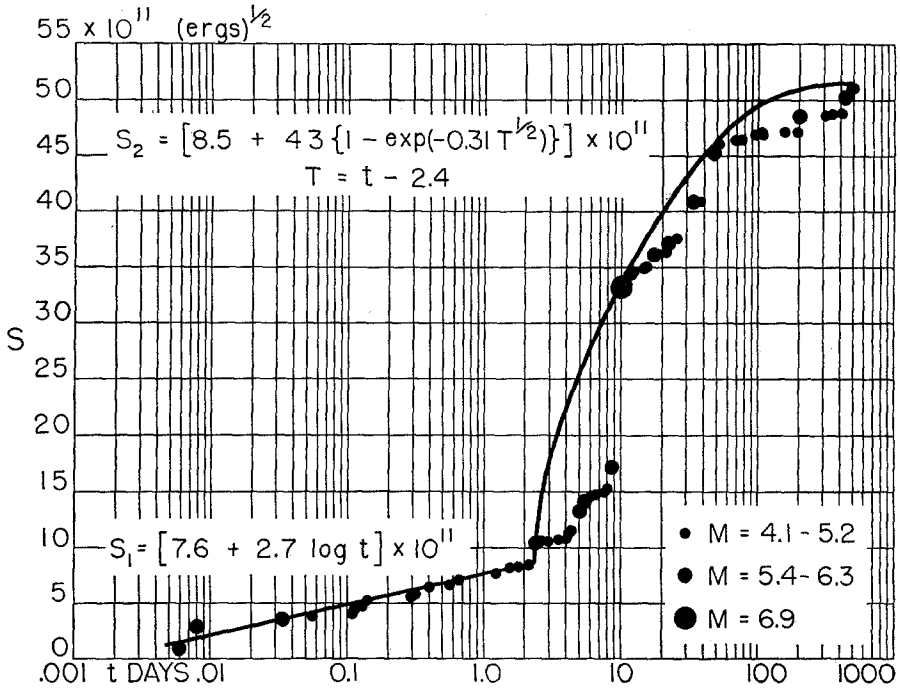

Fig. 16. Accumulated elastic strain rebound increments (times k) of the Hawke's Bay aftershock sequence.

Manix, California, Earthquake Aftershock Sequence

A sequence of aftershocks followed an earthquake of magnitude 6.2 which occurred on April 10, 1947, near Manix, California. The coördinates of the epicenter are $\phi = 34°\ 58'$ N, $\lambda = 116°\ 32'$ W. Magnitudes for this sequence were determined by Richter to January 3, 1949, 634 days from the time of origin of the principal shock. In figure 17, the accumulated sum of elastic strain rebound increments S is plotted on semilog coördinates. The points fall close to the straight line calculated from the equation

$$S = [19.4 + 6.4 \log t] \times 10^{10}\ (\text{ergs})^{\frac{1}{2}}, \qquad (20)$$

which is of the form of equations (2) and (3). This sequence therefore represents a compressional elastic creep with no appreciable shearing component.

Presumably this sequence is still active although there must eventually come a time when the interval between shocks is so large that the fault becomes cemented or locked and thus terminates the sequence.

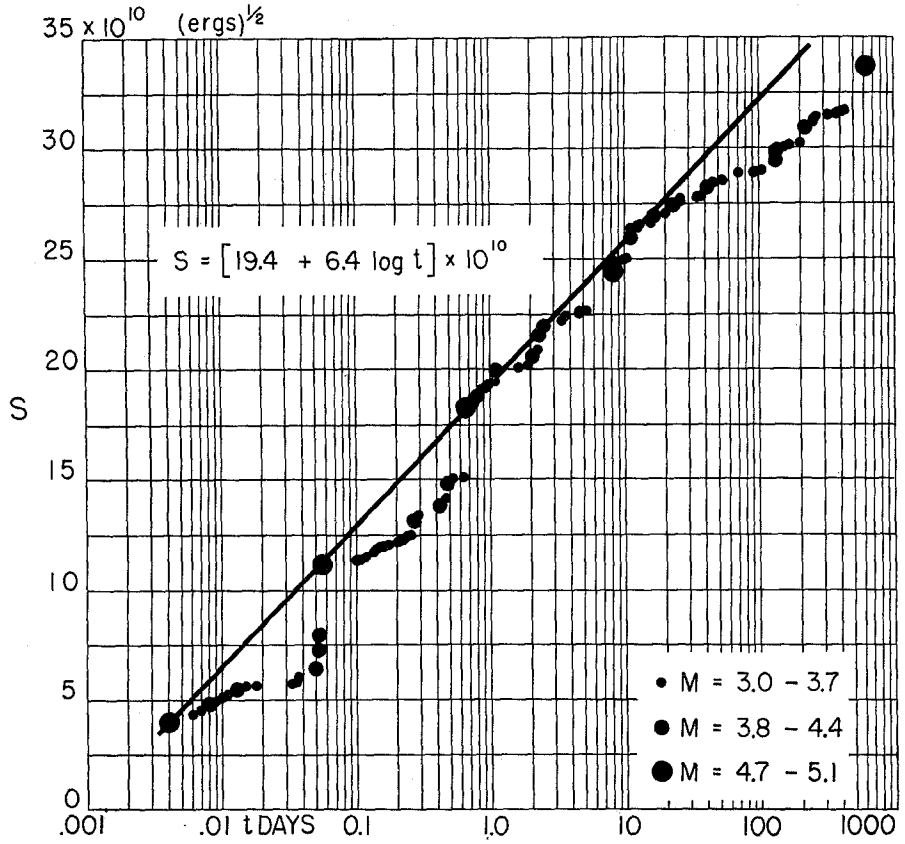

Fig. 17. Accumulated elastic strain rebound increments (times k) of the Manix aftershock sequence.

The points for shocks occurring after 10 days appear to depart systematically from the straight line. If this departure is not a result of accidental errors, it may be evidence for flow during the longer intervals of relaxation between shocks in this portion of the sequence. (See fig. 8.)

The total accumulated strain rebound (times k) for this sequence up to January 3, 1949, is 3.4×10^{11} (ergs)$^{\frac{1}{2}}$. The strain rebound (times k) which produced the principal shock was 3.8×10^{11} (ergs)$^{\frac{1}{2}}$. The ratio of elastic strain to creep strain at the time of the principal shock was not greater than 3.8/3.4

= 1.1. The seismic wave energy released in the aftershocks up to January 3, 1949, was 5.0×10^{22} ergs; that released in the principal shock was 1.5×10^{23} ergs. Since this sequence exhibited no shearing creep, it may be assumed that the strain pattern was so oriented as to provide compressional strains only. It would seem, therefore, that, in spite of the fact that the Manix epicenters lie in a region within 200 km. of the Long Beach epicenters, their fault-strain patterns were quite different.

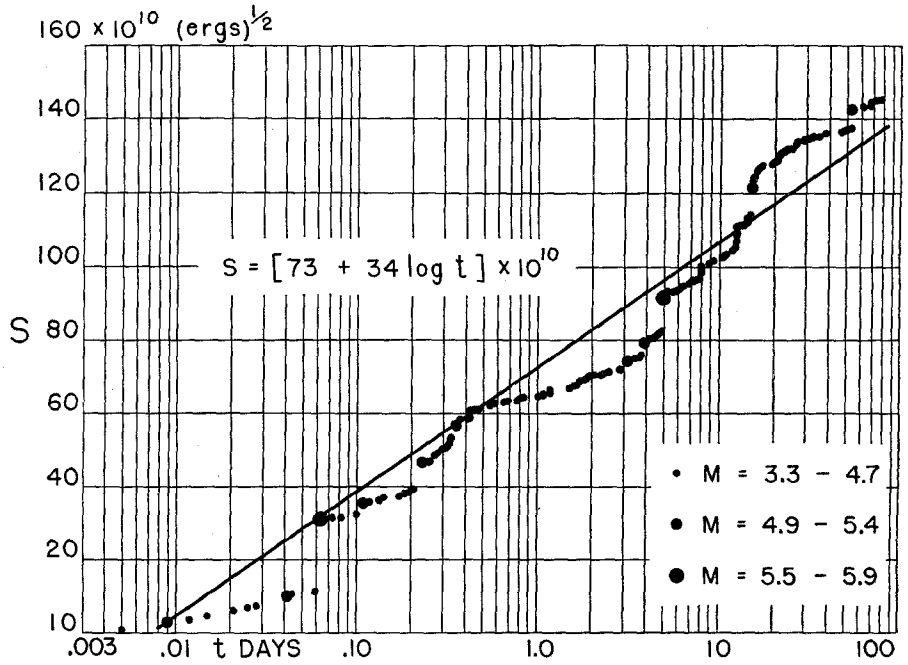

Fig. 18. Accumulated elastic strain rebound increments (times k) of the Nevada aftershock sequence of December 20, 1932.

Figure 18 shows a plot of S for the aftershock sequence of the Nevada earthquake of December 20, 1932 ($\phi = 38°.7$ N, $\lambda = 118°$ W; $M = 7.2$). Magnitudes for this sequence were determined by Richter for shocks up to December 22, 4:25, and those which followed were measured by Gilman. Measurements on this sequence were not carried beyond March 10, 1933, the date of the Long Beach earthquake, owing to difficulty in identifying the infrequent Nevada shocks on the disturbed seismograms resulting from the Long Beach sequence. The straight line in the figure was calculated from the equation

$$S = [73 + 34 \log t] \times 10^{10} \text{ (ergs)}^{\frac{1}{2}}, \tag{21}$$

which is characteristic of compressional elastic creep as defined by equations (2) and (3). At the time the measurements on this sequence terminated, the value of S_{max} was 1.4×10^{12} (ergs)$^{\frac{1}{2}}$. In the principal shock the elastic-strain rebound (times k) was $J_0^{\frac{1}{2}} = 3.2 \times 10^{12}$. The ratio of elastic strain to creep strain at the time of the principal shock was therefore not greater than $3.2 \times 10^{12}/1.4 \times 10^{12} = 2.2$. The energy released as waves in the principal shock and in the aftershocks was 1.0×10^{25} ergs and 7.1×10^{22} ergs, respectively. Assum-

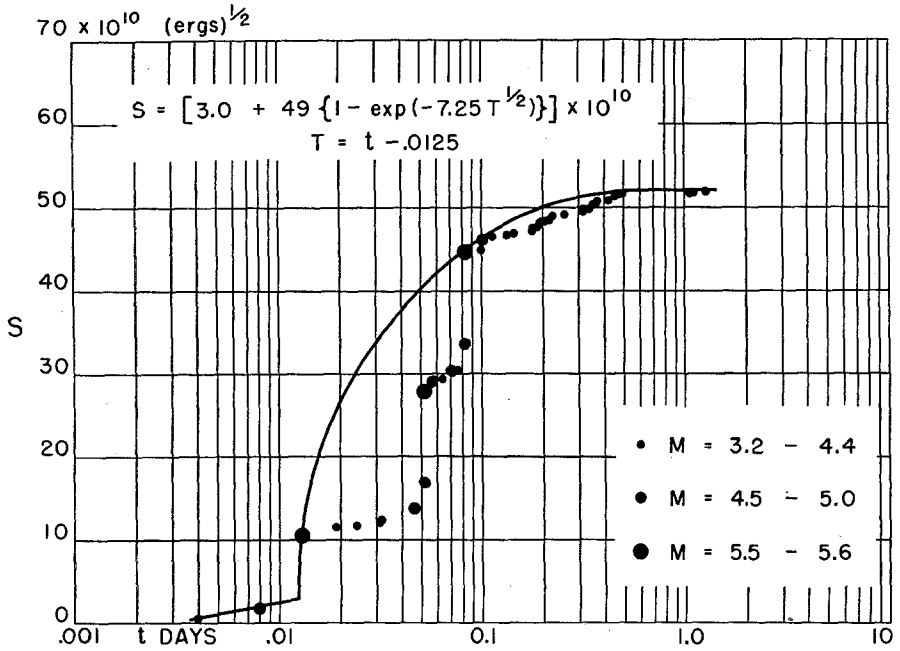

Fig. 19. Accumulated elastic strain rebound increments (times k) of the Imperial Valley aftershock sequence.

ing that the creep elastic element is linear, as was done in the case of the Long Beach sequence, the energy lost as heat in the creep mechanism during the aftershock sequence was

$$\frac{1}{2.2} \times 10^{25} = 4.5 \times 10^{24} \text{ ergs.}$$

Imperial Valley Sequence

In figure 19 a graph of S is shown for the aftershock sequence of the Imperial Valley, California, earthquake of May 18, 1940 ($\phi = 32°\ 44'$ N, $\lambda = 116°\ 30'$ W; M = 6.7). The magnitudes for this sequence were taken from the Bulletin of the Seismological Laboratory and were computed by Richter. Although the

scatter of the points is large, this sequence appears to present a case in which the creep strain recovery is nearly all in shear. The curve was drawn from values of S calculated from the equation

$$S = [3.0 + 49\{1 - \exp(-7.2T^{\frac{1}{2}})\}] \times 10^{10}\,(\text{ergs})^{\frac{1}{2}}, \tag{22}$$

which is of the form of equation given by Michelson for shearing creep recovery. This sequence was completed in approximately 1.5 days, the shortest recovery interval observed so far. This high rate of recovery may be respon-

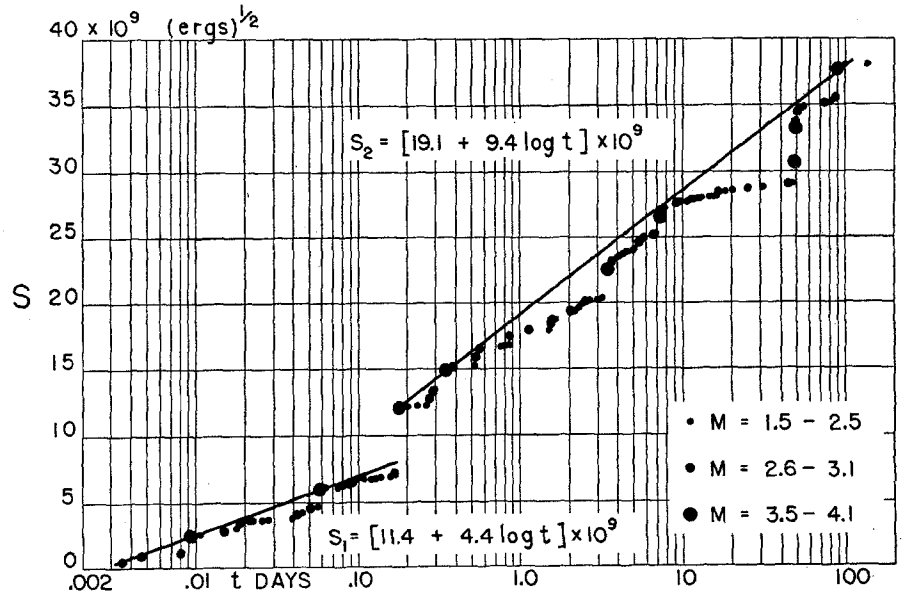

Fig 20. Accumulated elastic strain rebound increments (times k) of the Signal Hill aftershock sequence.

sible for the scatter of the points, since the scatter represents an irregularity in the times of origin of the aftershocks of only a few minutes. The value of S_{max}, the total accumulated rebound strain (times k) for this sequence, is 5.2×10^{11} (ergs)$^{\frac{1}{2}}$, as compared with 1.1×10^{12} (ergs)$^{\frac{1}{2}}$ for the principal shock. The ratio of the two is 2.1. The energy released in the aftershocks as waves was 3.7×10^{22} ergs, and that released in the principal shock was 1.3×10^{24} ergs. Hence the approximate value of energy stored in the creep strain was $1/2.1 \times 1.3 \times 10^{24} = 6.2 \times 10^{23}$ ergs, of which 5.8×10^{23} ergs was released as heat at an average power of 4.5×10^{8} kilowatts during the day and a half of aftershock activity.

Signal Hill Aftershock Sequence

Figure 20 shows a plot of the sequence of aftershocks following the Signal Hill, California, earthquake of October 2, 1933 ($\phi = 33° 47'$ N, $\lambda = 118° 08'$ W; M = 5.4). This earthquake occurred near or just beyond the northern limit of the epicenters of the Long Beach earthquake sequence. At the time of its occurrence there was an uncertainty concerning whether or not it was an aftershock of the Long Beach earthquake. This shock does not fall on the curve of S for the Long Beach aftershock sequence. Moreover, it was followed by a sequence of aftershocks of its own. It appears safe, therefore, to assume that it was an independent event. Magnitudes for this sequence were determined by Gilman to February 14, 1934. The observed values of S fall on two straight lines when plotted on semilog coördinates as shown. The first line is computed from the equation

$$S_1 = [11.4 + 4.4 \log t] \times 10^9, \tag{23}$$

and the second line from the equation

$$S_2 = [19 + 9.4 \log t] \times 10^9. \tag{24}$$

Both of these equations represent compressional creep without shear. The first phase ends and the second begins with the relatively large aftershock which occurred 0.18 day from the time of origin of the principal shock. The existence of the two phases must be associated in some manner with the mechanism of faulting. Perhaps it indicates an increase in the active area of faulting at the moment the rate changed. Although this sequence was initiated by the smallest principal earthquake and comprised the lowest aftershock magnitudes of this study, nevertheless it was observed for 136 days, and presumably activity continued for some time thereafter. The maximum observed value of S for the sequence was $S_{max} = 3.8 \times 10^{10}$ (ergs)$^{\frac{1}{2}}$. The corresponding value of $J_0^{\frac{1}{2}}$ of the principal shock was 7.1×10^{11}. The ratio of the two is 0.53. Assuming a linear creep-elastic element, the ratio of energy stored in the creep mechanism to that released in the principal earthquake was also $S_{max}/J_0^{\frac{1}{2}} = 0.53$. The energy released in the aftershocks as waves was greater than 5.7×10^{19} ergs. The energy released in the principal shock as waves was 5.0×10^{21} ergs. Thus, only about 2 per cent of the potential creep energy appeared as waves. The rest, approximately 2.5×10^{21} ergs, was dissipated as heat in the rocks.

In table 3 the data concerning strain and energy for the sequences is summarized. M is the magnitude of the principal earthquake. J_0 is the energy released by the principal earthquake in the form of seismic waves. $\sum J_i$ is the

TABLE 3

COMPARISON OF MAGNITUDES AND ENERGY RELATIONS OF EARTHQUAKE SEQUENCES STUDIED

Principal earthquake	M	J_0 ergs	ΣJ_i ergs	$J_0^{1/2}$ $(\text{ergs})^{1/2}$	S_{max} $(\text{ergs})^{1/2}$	R	r
Hawke's Bay, Feb. 3, 1931	7.6	5.0×10^{25}	3.1×10^{24}	6.9×10^{12}	5.1×10^{12}	0.06	0.74
Nevada, Dec. 20, 1932	7.2	1.0×10^{25}	7.2×10^{22}	3.2×10^{12}	1.4×10^{12}	0.007	0.45
Long Beach, March 10, 1933	6.25	1.8×10^{23}	2.4×10^{22}	4.3×10^{11}	9.9×10^{11}	0.13	2.3
Signal Hill, Oct. 2, 1933	5.4	5.0×10^{21}	5.7×10^{19}	7.1×10^{10}	3.8×10^{10}	0.011	0.55
Imperial Valley, May 18, 1940	6.7	1.3×10^{24}	3.7×10^{22}	1.1×10^{12}	5.2×10^{11}	0.028	0.47
Manix, April 10, 1947	6.2	1.5×10^{23}	5.0×10^{22}	3.8×10^{11}	3.4×10^{11}	0.3	0.89

total energy released by the aftershocks in the form of seismic waves. $J_0^{\frac{1}{2}}$ is the elastic strain rebound (times k) of the principal earthquake. $S_{\max}$ is the sum (times k) of the elastic strain rebound increments of the aftershocks. The ratio of total aftershock wave energy to the energy of the principal earthquake is $R = \sum J_i/J_0$. The ratio of total elastic rebound strain for the aftershocks to that of the principal shock is indicated by $r = S_{\max}/J_0^{\frac{1}{2}}$. If the relation between creep stress and creep strain is assumed to be linear, r also represents the ratio of energy stored in the creep mechanism to energy stored in the elastic element of the fault rock just before the occurrence of the principal earthquake.

Conclusion

Evidence has been presented indicating that aftershocks are produced by creep of the fault rocks. The creep may be purely compressional, purely shearing, or a combination of the two. When the two occur in combination, the compressional phase occurs first. The shearing phase follows after an interval, which in the sequences studied in this investigation varied from 0.01 to 2.4 days. Apparently the shearing phases are all produced by creep recovery. In the compressional sequences and phases the observed data do not provide sufficient information to distinguish between forward creep and creep recovery. Consequently, although it has been assumed in this paper that the compressional phases represent creep recovery, it must be recognized that they may be produced by forward creep. In sequences having both compressional and shearing phases, the compressional phases, although still at a high level of activity, always terminated abruptly with the onset of the shearing phase. It appears, therefore, that a substantial part of the compressional creep in these phases was blocked in some manner, or that it continued active without producing earthquakes, perhaps as a result of reduced normal stress on the fault surfaces.

Sequences exhibiting shearing creep approached fairly definite terminations in time intervals which varied from 1.5 to 500 days. There appears to be no relation between the duration of aftershock activity and the magnitude of the principal earthquake. Presumably it is a function of the creep time constant only of the fault rock. The purely compressional creep sequences were observed for intervals varying from 70 to 640 days. None appeared to have a definite termination.

Using fairly reasonable assumptions, the value of the energy released in the creep mechanism of the rocks as seismic waves and heat was calculated roughly for each of the sequences. It varied from approximately 0.5 to 2.0 times the energy released in the purely elastic elements as seismic waves. Of the total energy released in the aftershock sequences only approximately 1 to 5 per cent appeared in the form of seismic waves. The remainder was liberated as heat in the fault rocks. If this quantitative relation between creep energy and

elastic energy should prove to be general, it will be necessary to take the creep energy into account when estimating the total energy released by seismic processes. The ratio of elastic creep strain to elastic strain in the fault rocks preceding the principal earthquakes varied from 0.5 to 2.0 in the different sequences.

The smoothness of the elastic rebound increment curves provides evidence for the precision and usefulness of the revised magnitude scale of Gutenberg and Richter. Absolute values of energies derived from the scale may be in error by a factor of 10, or possibly 100, as pointed out by its authors, but the relative values of the square roots of the energies upon which the forms of the curves depend are evidently much more precise.

CALIFORNIA INSTITUTE OF TECHNOLOGY
PASADENA, CALIFORNIA
(Division of Geological Sciences, contribution no. 519)